Covid CNN–SVM: Automated Categorization of Novel Coronavirus Disease from X-Ray Images

Israa Rafaa Abdulqader*

Computer Science and Mathematics College, Tikrit University, Iraq.

*Corresponding Email: *israa.r.abdalkader@tu.edu.iq*

Abstract: In the computer-aided diagnostic (CAD) system, automated Coronavirus infection disclosure plays a crucial role in early identifying positive patients to prevent the disease from spreading further. The advent of algorithms for deep learning and machine learning has tackled classification tasks with promising results, especially in classifying images. However, the small size of the databases for medical images is a limitation associated with train deep neural networks. We use a combination of convolutional neural network (CNN) features and a support vector machine (SVM) for X-ray image classification to overcome this problem. This research work used CNN methods to extract features from 1,338 Chest X-ray frontal view image data. An SVM is used with CNN features to classify images in two classes: COVID-19 and Normal cases for enhanced performance. We conducted and evaluated our experiments on several public databases, which have been used in the recently published articles. The performance of the proposed method revealed accuracy, AUC, sensitivity, specificity of 0.995, 0.999, and 0.995 for classification, respectively. The high performance of the detection system achieved in this research reveals the effectiveness of deep features and the machine learning classifier approach for detecting COVID-19 cases using X-ray images. This would be extremely helpful in accelerating disease diagnosis with the available resources.

Keywords: COVID-19, Transfer Learning, Deep Learning, Machine Learning, Feature Extraction X-Ray.

1. INTRODUCTION

Newly discovered Coronavirus pneumonia, also referred to as COVID-19, is highly contagious. The Coronavirus was first recorded around the end of 2019 in the Chinese city of Wuhan. By February 05, 2021, there have been more than 103,989,900 confirmed cases of COVID-19, including 2,260,256 recorded deaths worldwide [1]. Studies have shown

that, with a generative rate between 2.24 and 3.58, the virus`s transmission rate (TR) is highly dangerous, which is incredibly higher than any other form of viral flu [2]. As there are no known vaccines or medications, the treatment for this viral infection is asymptomatic and a supportive cure [3]. COVID-19 greatly impacts the health, social and economic lives of people worldwide [4].

For these reasons, a great deal of research is being conducted on early diagnosis coronavirus disease intervention. Early diagnosis is of real significance because of the unavailability of clinical medication or vaccination for novel COVID-19 disease to isolate the suspected person quickly and reduce the risk of infection to a healthy population [5]. Due to the absence of dependable automated toolkits, there has been an increasing need for supplementary diagnostic tools. Recent radiological imaging studies have revealed significant COVID-19 virus features within the pictures [6]. Health care workers have identified an alternate and more sensitive screening technique, such as a CT scan or chest x-ray imaging, which can provide visible indicators of viral COVID-19 infection [7,8]. Research has demonstrated that COVID-19 affects the patient's lungs and that its symptoms are visible in X-ray or CT scans.

The use of advanced artificial intelligence (AI) techniques integrated with radiological imaging can effectively identify this virus [9]. The utilisation of machine learning techniques for automated diagnosis in medicine has recently garnered attention as a supplementary approach for physicians [10]. Deep learning is a famous field of artificial intelligence (AI) that enables the creation of algorithms that may produce desired results utilising input data, without the requirement for manual feature extraction. [11]   Several problems, including the identification of arrhythmia [12], detection of skin cancer [13], identification of breast cancer [14], categorization of brain diseases [15], and detection of pneumonia [16], have been effectively applied and developed using deep learning approaches. Efficient, precise, and rapid AI models can thus aid in resolving this problem and rapidly aid patients. Despite the vital role played by radiologists, who possess substantial experience in the field, the implementation of Radiological AI technology can significantly enhance the accuracy of diagnoses [17].

Using radiological imaging have become increasingly common for the detection of COVID-19. The author introduced a hybrid architecture in [18] that incorporates artificial intelligence, specifically machine learning and deep learning techniques, to identify COVID-19 patients by analysing chest X-ray pictures. In addition, the researchers in [19] presented the utilisation of deep learning with CT scans for COVID-19 detection. Their empirical results demonstrated that ResNet101 exhibited superior performance compared to other approaches in evaluating 194 patients, achieving an area under the curve (AUC) of 0.99 across 1020 CT scans.

Related work
In a study with binary or many categories, COVID-19 is detected using chest X-rays. In some studies, raw data is used, whereas, in others, feature extraction is employed. The

number of data points used in the study also varies, and Convolutional neural networks are the most popular approach.

ResNet50, InceptionV3 and Inception-ResNetV2 were applied by the authors in [20], using transfer learning to classify X-ray images into normal and COVID-19 classes. With ResNet50, this approach achieved good performance with an accuracy of 96%. Nevertheless, the quantity of X-ray images is merely 100, indicating a restricted number of samples. In [21], an automatic detection method of COVID-19 cases from the X-ray images was proposed. An accuracy of 98.08 % was reported for binary classification and 87.02 % for multi-class classification into COVID-19, normal and pneumonia. In [22], the authors investigated the use of deep learning models to detect COVID-19 patients from X-ray pictures. Five hundred X-rays from publicly available datasets trained DenseNet-121, SqueezeNet, ResNet18, and ResNet50. The detection system has a sensitivity of 98 per cent and a specificity of about 90 percent. However, a limited handful of COVID-19 pictures were used in the experiments. As a result, further experiments on a larger collection of neatly labelled COVID-19 pictures are required for a more credible assessment of these models' accuracy. The CVOIDX-Net was designed to diagnose coronavirus using 2-D X-ray pictures. Fifty chest X-ray pictures were used to verify the study, with 25 confirmed positive COVID-19 patients. However, the obtained accuracy was 90%, which is insufficient to rely on the diagnostic system. In [23], a COVID-19 and other forms of pneumonia with unique localisation from chest X-rays are identified using a deep neural network architecture called CovXNet. To detect anomalies in X-rays from various viewpoints, depthwise convolution is employed with varied dilation rates to combine information from various receptive fields. Two different datasets were used in the experiments, and the diagnostic performance was about 90% accuracy. However, a total of 305 COVID-19 X-ray images and 305 Normal X-ray images were utilized. Hence, additional examinations on a more extensive collection of COVID-19 photographs are imperative to ensure a more dependable evaluation of the accuracy of the system.In [24], the automated diagnosis of Coronavirus disease was proposed. The authors utilise X-ray pictures obtained from patients who have been confirmed to have COVID-19, pneumonia, and normal health conditions. COVID-19 diagnosis was conducted using the Transfer Learning method, utilising limited X-Ray image datasets. The results obtained from detecting COVID-19 diseases using deep X-ray learning are 96.78%, 98.66%, and 96.46% of accuracy, sensitivity, and specificity, respectively. However, the number of samples used in this work is imbalanced. In [25], a deep learning model was used to propose a system for diagnosing Coronavirus. The data classes were reorganised as a preprocessing phase in this study using the Fuzzy Color method. The pictures that were structured with the original photos were stacked. The stacked dataset was then trained using deep learning models namely MobileNetV2, and SqueezeNet to extract features. using the Social Mimic optimization technique was processed the feature sets acquired. Finally, Support Vector Machines were used to classify the X-ray imagery to a coronavirus, pneumonia, and normal. The proposed technique yielded an overall categorization rate of 98.25 percent. However, only 65 X-ray images of COVID-19 are used in this study, which is very few. In addition, the number of samples of the dataset is imbalance

Although researchers have conducted considerable studies to diagnose COVID-19 using radiological scans, there is yet untapped potential for additional comprehensive investigations and advancements. This work proposes a diagnostic intelligence model for COVID-19 infection diagnosis based on the convolution neural networks (CNN). The proposed model introduces an end-to-end learning framework that can learn discriminatory features extracted directly from the Chest X-ray images.

In The Present Study, The Key Contributions Are:
1. There is no data imbalance.
2. The model has been trained using a considerable number of X-ray coronavirus chest images compared to previous studies.
3. The suggested model is a fully automated diagnostic technique that does not involve the previous extraction of characteristics.
4. Comprehensive tests prove the coupling of a CNN with the SVM classification to get high classifying performance for COVID-19 data.

Developed System
The proposed methodology for diagnosing COVID-19 based on X-ray pictures, as depicted in Fig.1, consists of two phases: the Data Pre-processing phase and the training phase of Convolutional Neural Networks. This study classified the CXR images into two classes as COVID-19 and normal. Description of the system phases is discussed as follows.
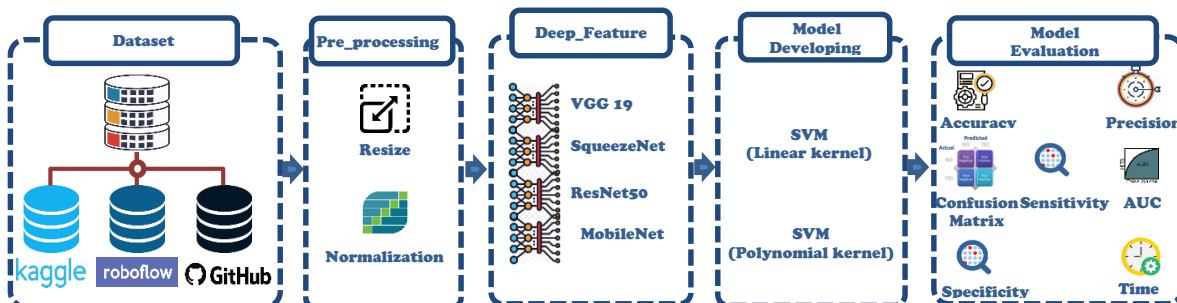

Fig. 1. The diagram of the proposed automatic COVID-19 diagnosis

1.1. Dataset
Seven public data sets are the primary source for chest X-ray (CXR) pictures. CXR pictures of COVID-19 patients and healthy people were selected. Dr. Joseph Cohan generates the first GitHub public data collection. CXR images of COVID-19 positive patients, significant ARS, MARS, and ARDS are included. In this collection, 340 images include CXR frontal, non-frontal, and CT scans. The second GitHub dataset, "X-Ray (Pneumonia)", has 55 COVID-19 Chest X-rays. The "Chest X-Ray Images" data set is obtained from the Kaggle repository as a third dataset, consisting of CXR images of both Pneumonia Patients and Normal persons [26]. The fourth dataset from Kaggle comprises 5679 chest X-ray (CXR) images categorised into two classes: normal and pneumonia. The fifth dataset, known as the COVID-19 Radiography dataset, consists of 2905 CXR images, including both frontal and non-frontal views. The images are categorised into three

classes: Viral Pneumonia, COVID-19, and Normal.   The chest X-ray image is sourced from the sixth dataset available in the Kaggle repository specifically designed for the purpose of diagnosing COVID-19. 174 CXR images of positive and non-positive coronavirus patients are included. COVID-19 X-rays have 280 CXRs for both COVID-19 and normal cases. We conclude with Robofow's COVID-19 and Pneumonia X-ray datasets, which include 199 COVID-19 images and 1965 Healthy.

For this study, only frontal X-rays of patients who tested positive for COVID-19 and patients without the virus were chosen. X-rays taken from non-frontal angles, CT scans, and X-rays of patients with non-COVID-19 disorders were excluded.   Furthermore, an equal amount of photos are used in each class to address the issue of data imbalance. Hence, the ultimate dataset has 1,338 photos, with an equal distribution of 669 images for both COVID-19 patients and normal cases.

1.2. Pre-processing Data

COVID CXR pictures from GitHub and Kaggle sources have dimensions ranging from 508×500 to 4248×3480 pixels.   In the experiment, we set the photo size to 224×224 pixels.   Keras' built-in "preprocess input" function converts and resizes the input image to model specifications.

1.3. Deep Feature

An essential aspect in the process of training a machine to provide reliable outcomes from raw input data is the precise extraction of features. The deep extraction method based on pre-trained CNN models is known as deep transfer learning (DTL). (DTL) involves transferring information from a source domain, which has been taught using a large number of training samples, to a target domain that has comparatively fewer data. With the assistance of an extensive dataset of the source domain, effective image classification can thus be accomplished. DTL refers to the process of transferring certain layers of a pre-trained CNN model, which has been previously trained using of millions of images, from perspective of deep learning. According to the study [26], the CNN model's task-dependent layers, such as the fully connected and classification output layers, are excluded from the network architecture. The remaining layers are saved for the current classification task application.

In this work, the input photos are encoded into a feature vector using DTL models. Different DTL architectures, including as VGG 19, SqueezeNet, ResNet50, and MobileNet, were chosen for feature extraction [27]. The encoded feature vectors are input into an SVM algorithm to obtain the final prediction.

1.4. Model Developing

SVM is an efficient classifier that Vapnik develops for optimization [28]. SVM is simply the coordinates of individual observation. SVM performs data categorization by creating an optimal hyperplane in N-dimensional space, which splits data samples into positive and negative [29]. SVM minimizes the possibilities of overfitting because it is a global representation of the data samples [22]. In SVM, the kernel and two crucial parameters are

cost (c) and gamma (γ). Cost controls the trade-off between training and testing accuracy. Gamma controls the effect of a single training data sample.

Provided the feature vector xi, weight vector w, and class label yi

$$\text{Minimize}: \frac{1}{2}\|w\| + C\left(\sum_i \xi_i\right) \tag{1}$$

$$\text{Subject to}: y_i(w^T x_i + w_0) \geq 1 \tag{2}$$

where i denotes the number of samples, C denotes the cost parameter, and ξ denotes the training errors.

1.5. Evaluation Criteria

In the current study, five evaluation criteria were used to evaluate the proposed model. Criteria refer to the various measurements from which the alternatives can be evaluated and benchmarked. Fig.2 illustrates the whole set of criteria employed in this study.
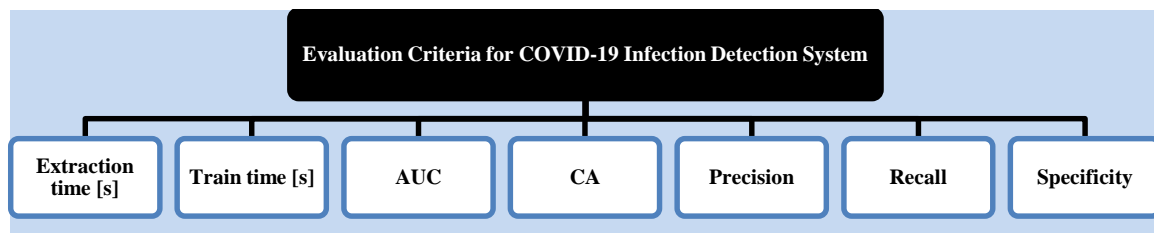

Fig. 2. Evaluation criteria used to evaluate the detection framework performance

The study utilised five criteria to assess the performance of the model: classification accuracy (CA), Area Under the Curve (AUC), precision, specificity, and recall. These metrics are commonly employed and have been previously documented [32]. The criteria are formulated and presented in the following manner:

Classification Accuracy (CA) is a primary metric for assessing classification models and quantifies the level of agreement with the true value. The accuracy is determined by applying the following formula. The accuracy is calculated by dividing the number of successfully identified samples by the total number of samples.

$$CA = \frac{TP+TN}{TP+FP+FN+TN} \tag{3}$$

TP is the number of correctly identified positive samples, TN is the correctly detected negative sample, and FP is the number of positive-categorised negative cases. FN is the number of negative positives.

Sensitivity: number of positive samples correctly recognised. High sensitivity means few FN samples, hence fewer TP samples are missed. Formula for sensitivity:

$$Recall = \frac{TP}{TP+FN} \qquad (4)$$

Precision is the proportion of detected samples that were correctly identified. It evaluates the classifier's irrelevant subject rejection. This formula calculates precision

$$Precision = \frac{TP}{TP+FP} \qquad (5)$$

The metric of specificity, often known as the true negative rate, evaluates a model's capability to correctly identify true negatives for each category. Specificity in COVID-19 detection refers to the test's capacity to accurately identify individuals who do not have the disease. A high specificity rating indicates a low occurrence of false positive findings. The equations for computing the Specificity metric are provided below.

$$Specificity = \frac{TN}{TN+FP} \qquad (6)$$

Receiver Operating Characteristics (ROC) and AUC assess categorization model performance at different threshold setups. AUC measures class-specific model performance ((i.e. a degree of separability). Higher the AUC is better.

2. RESULTS AND DISCUSSION

Extracting features from radiographs for training machine learning models is essential since model performance is affected by the quality of the extracted features. This study employed transfer learning techniques, specifically utilising four pre-trained convolutional neural network models: VGG 19, SqueezeNet, ResNet50, and MobileNet. The purpose was to compute a feature vector for each X-ray picture of the Chest. The resulting feature vector is inputted into an SVM, which is a widely used supervised learning technique, in order to classify the X-ray pictures.

The purpose of this research is to study the classification of COVID-19 pneumonia from an X-ray image of the Chest using features extracted by pre-trained CNN models and the SVM algorithm. The SVM classifier has been implemented with two kernel functions: Polynomial and Linear. For classification purposes. Experiments are carried out on a Windows-based computer system with 2.50 GHz Intel(R) Core (TM) i5, 8.0 GB RAM and a 2 GB graphics processing device in a Python environment using the Keras and

TensorFlow2 packages (GPU). Table 1 summarises the findings of SVM's linear-kernel performance evaluation metrics for the extracted feature of deep CNNs.

Table 1. The proposed SVM Linear kernel obtained performance results.

Model	AUC	CA	Precision	Recall	Specificity
VGG 19	1	0.993	0.993	0.993	0.993
SqueezeNet	1	0.995	0.995	0.995	0.995
ResNet50	1	0.99	0.99	0.99	0.99
MobileNet	0.909	0.832	0.832	0.832	0.832

In terms of accuracy presented in Table 1, the SqueezeNet architecture obtained the top result with a maximum value of 99.5%. The second-best result obtained by VGG19 function extraction with 99.3% accuracy is also inferred from Table 2. However, the remaining scales still have high values in the 99% and 98% range, which indicates the model's effectiveness in distinguishing between true positive and negative. The results also showed that the lowest rating provided by the MobileNet model had an accuracy of 83.2%. As given in Table 2, the highest precision, recall, and specificity rates are produced by SqueezeNet architecture with the value of 99.5% of precision, recall, and specificity. The MobileNet feature vector yielded the lowest results with values of (83.2, 83.2, and 83.2) percentage precision, recall, and specificity rates. Table 2 also indicates that four models produced very high AUC values in 1 range, except MobileNet, which yielded 0.909. Table 2 illustrate the performance of SVM with a Polynomial kernel.

Table 2. Performance results were obtained by classification X-ray images using SVM with the polynomial kernel.

Model	AUC	CA	Precision	Recall	Specificity
VGG 19	0.998	0.934	0.941	0.934	0.933
SqueezeNet	0.999	0.939	0.945	0.939	0.939
ResNet50	0.999	0.983	0.983	0.983	0.983
MobileNet	0.949	0.748	0.822	0.748	0.746

As given in Table 2, the best accuracy rate was 98.3% resulted in ResNet50 architecture.. The models VGG 19 and SqueezeNet also produced very high accuracy of about 93.9% and 93.4%, respectively. Conversely, MobileNet architecture obtained the lowest accuracy rate of about 74.8%. Concerning AUC, All models produced excellent AUC values in a range of 94.9% to 99.9%. In terms of Precision, Recall, and Specificity, all models except MobileNet have high scores, which means that the network has false positives with a low probability of occurrence.

The confusion matrix is another effective metric that benefits to measure classification performance. Thus, the classification outcome of the proposed approach is represented using a confusion matrix. Each entry in the confusion matrix matches the desired label against the predicted diagnostic system output. Tables 3 and 4 show the confusion matrices

of the features extracted by six deep CNN architectures trained by SVM with a linear and polynomial.

Table 3. Confusion matrices of six deep networks and SVM linear kernel include the number of samples, training proportion, and predicted proportion.

confusion matrix / Feature Model	Predicted						class	
	Number of Instances		Proportion of Actual		Proportion of Predicted			
	COVID	Normal	COVID	Normal	COVID	Normal		
VGG 19	659	3	99.5%	0.5%	99.1%	0.5%	COVID	
	6	663	0.9%	99.1%	0.9%	99.5%	Normal	
SqueezeNet	664	5	99.3%	0.7%	98.8%	0.8%	COVID	
	8	661	1.2%	98.8%	1.2%	99.2%	Normal	
ResNet50	656	6	99.1%	0.9%	99.8%	0.9%	COVID	Actual
	1	668	0.1%	99.9%	0.2%	99.1%	Normal	
MobileNet	543	119	82.0%	18.0 %	83.8%	17.4%	COVID	
	105	564	15.7 %	84.3 %	16.2%	82.6%	Normal	

Table 4. Confusion matrices of six deep networks and SVM polynomial kernel include the number of samples, proportion of training, and predicted proportion.

confusion matrix / Feature Model	Predicted						class	
	Number of Instances		Proportion of Actual		Proportion of Predicted			
	COVID	Normal	COVID	Normal	COVID	Normal		
VGG 19	577	85	87.2 %	12.8 %	99.5 %	11.3 %	COVID	
	3	666	0.4 %	99.6 %	0.5 %	88.7 %	Normal	
SqueezeNet	582	80	87.9 %	12.1 %	99.8 %	10.7 %	COVID	
	1	668	0.1 %	99.9 %	0.2 %	89.3 %	Normal	
ResNet50	583	79	88.1 %	11.9 %	99.8 %	10.6 %	COVID	Actual
	1	668	0.1 %	99.9 %	0.2 %	89.4 %	Normal	
MobileNet	651	18	97.3 %	2.7 %	99.2 %	2.6 %	COVID	
	5	664	0.7 %	99.3 %	0.8 %	97.4 %	Normal	

Table 5. Feature extraction time of six deep CNN models and training time of SVM per kernel.

Model	Extraction Time [s]	Training Time [s]	
		Linear	Polynomial
VGG 19	358.7	100.352	120.155
SqueezeNet	184.95	79.863	65.12
ResNet50	255.175	37.532	23.678
MobileNet	223.25	6.972	8.286

In Table 5 the total extraction time for 1,338 images using VGG-19 architectures was estimated at 358.7s and is the longest extraction of visual features. While SqueezeNet was the fastest visual feature extractor by 184.95 seconds. As less time-consuming, the MobileNet model took 223.25 seconds for the feature extraction phase and 6.972 seconds for the training phase on the SVM classifier with the Linear kernel. The MobileNet architecture and SVM classifier with the Polynomial kernel consumed the second least time to classify the X-ray images of about 231,536 seconds. Comparing the time consuming with the accuracy obtained, SqueezeNet model and SVM with the linear kernel is the best method yielded 99.5% accuracy within 264.813 seconds. To conclude, the extraction and training period for the technique presented is astonishingly short comparing to training the CNN deep model, meaning that processing time is faster and resources are less utilised.

The system yielded 99.5%, proving that the technique is efficient. The high AUC value shows the system's ability to discriminate between positive COVID-19 and negative COVID-19.

Comparative Study with the Literature

Benchmarking is used for comparing the proposed model to previous work based on specific topics. Table 6 lists the essential previous research on diagnosing COVID-19 using X-ray pictures and an evaluation and comparison of the proposed model. Several key elements are indicated to be contrasted based on the direction of the provided issue. To sum up, the present work highlights the most critical challenges in COVID-19 research. In Table 6, CXR-based studies for COVID-19 detection are utilised as an alternative to benchmarking in terms of accuracy, sensitivity and specificity, which are the criteria for evaluation.

Table 6. Comparison of our model with state-of-the-art COVID-19 diagnosis models.

Study	Technique	Number of Samples				ACC (%)	SEN. (%)	SPE. (%)
		Normal	COVID-19	Pneumonia	Total			
Ali Narin [20]	ResNet50, InceptionV3 and Inception-ResNetV2	2800	100	2772	2872	96.1	-	98.2

Tanvir Mahmud [23]	CovXNet	305	305	305	915	90.3	89.9	89.1
Ioannis D. postolopoulos [24]	VGG19, MobileNet, Inception, Xception, Inception, ResNetV2	504	224	700	1427	96.7	99.1	-
Mesut Toğaçar [25]	SqueezeNet & MobileNetV2 (Combined Features Set)	295	65	98	458	98.25	97.96	98.61
Tulin Ozturk [21]	DarkNet	500	125	-	625	98	-	-
Shervin Minaee [22]	Deep-COVID	500	100	-	600	-	97.5	90
Proposed		669	669		1,338	99.5	99.5	99.5

As shown in Table 6, the accuracy attained by comparable works ranged from 90.3 % to 98.25 %. In comparison, the proposed work achieved 99.5% accuracy, which is the best accuracy obtained. Furthermore, most prior research studies used a small number of pictures for training and testing diagnosis systems. In contrast, the current study used a dataset of 1,338 images. Compared to similar studies, our dataset has a more significant number of samples.

3. CONCLUSION

An early diagnosis of COVID-19 is important to interrupt human-to-human transmission and patient treatment. Currently, isolation and quarantine are the most successful ways of delaying the spread of COVID-19. Chest X-ray imaging is vital for diagnosing diseases, monitoring disease development, and the severity of COVID-19 positive patients as successful diagnostic methods. This study offers a supported diagnosis of COVID-19 by utilising deep-learning models to extract features and machine learning techniques for classification. The suggested system underwent evaluation utilising several metrics including precision, sensitivity, specificity, and execution time for both the extraction and training data. The results demonstrate that our system outperformed multiple existing COVID-19 detection methods.

The results of this study will aid in the development of more specialised diagnostic and detection tools to combat the coronavirus pandemic, as well as the implementation of efficient and reliable diagnostic tools that use imaging data and intelligent approaches. Further investigations will be conducted in the future to study additional COVID-19 chest X-ray pictures and different deep Convolutional Neural Network (CNN) models for the purpose of identifying COVID-19. Furthermore, we shall explore various respiratory conditions.

4. REFERENCES

1. w. h. organization. (2021/2/4). WHO Coronavirus Disease (COVID-19) Dashboard. Available: https://covid19.who.int/?gclid=Cj0KCQiA0 6ABhDMARIsAFVdQv_cdCY-LtXxDV9YdFUMWjpCeWrqtBd-upOt4ERyJMSoL0nnfJFvFuEaAhSKEALw_wcB

2. A. J. Bokolo, "Application of telemedicine and eHealth technology for clinical services in response to COVID‑19 pandemic," Health and Technology, vol. 11, pp. 359-366, 2021.

3. C. Liu, Q. Zhou, Y. Li, L. V. Garner, S. P. Watkins, L. J. Carter, et al., "Research and development on therapeutic agents and vaccines for COVID-19 and related human coronavirus diseases," ed: ACS Publications, 2020.

4. F. Demir, A. Sengur, and V. Bajaj, "Convolutional neural networks based efficient approach for classification of lung diseases," Health information science and systems, vol. 8, pp. 1-8, 2020.

5. M. Ahmed, Z. Al-qaysi, M. L. Shuwandy, M. M. Salih, and M. H. Ali, "Automatic COVID-19 pneumonia diagnosis from x-ray lung image: A Deep Feature and Machine Learning Solution," in Journal of Physics: Conference Series, 2021, p. 012099.

6. M. M. Rahaman, C. Li, Y. Yao, F. Kulwa, M. A. Rahman, Q. Wang, et al., "Identification of COVID-19 samples from chest X-Ray images using deep learning: A comparison of transfer learning approaches," Journal of X-Ray Science and Technology, pp. 1-19, 2020.

7. Y. Li and L. Xia, "Coronavirus disease 2019 (COVID-19): role of chest CT in diagnosis and management," American Journal of Roentgenology, vol. 214, pp. 1280-1286, 2020.

8. G. D. Rubin, C. J. Ryerson, L. B. Haramati, N. Sverzellati, J. P. Kanne, S. Raoof, et al., "The role of chest imaging in patient management during the COVID-19 pandemic: a multinational consensus statement from the Fleischner Society," Chest, 2020.

9. J. D. López-Cabrera, R. Orozco-Morales, J. A. Portal-Diaz, O. Lovelle-Enríquez, and M. Pérez-Díaz, "Current limitations to identify COVID-19 using artificial intelligence with chest X-ray imaging," Health and Technology, vol. 11, pp. 411-424, 2021.

10. O. Faust, Y. Hagiwara, T. J. Hong, O. S. Lih, and U. R. Acharya, "Deep learning for healthcare applications based on physiological signals: A review," Computer methods and programs in biomedicine, vol. 161, pp. 1-13, 2018.

11. A. Krizhevsky, I. Sutskever, and G. E. Hinton, "Imagenet classification with deep convolutional neural networks," Advances in neural information processing systems, vol. 25, pp. 1097-1105, 2012.

12. Ö. Yıldırım, P. Pławiak, R.-S. Tan, and U. R. Acharya, "Arrhythmia detection using deep convolutional neural network with long duration ECG signals," Computers in biology and medicine, vol. 102, pp. 411-420, 2018.

13. A. Esteva, B. Kuprel, R. A. Novoa, J. Ko, S. M. Swetter, H. M. Blau, et al., "Dermatologist-level classification of skin cancer with deep neural networks," nature, vol. 542, pp. 115-118, 2017.

14. Y. Celik, M. Talo, O. Yildirim, M. Karabatak, and U. R. Acharya, "Automated invasive ductal carcinoma detection based using deep transfer learning with whole-slide images," Pattern Recognition Letters, vol. 133, pp. 232-239, 2020.

15. M. Talo, O. Yildirim, U. B. Baloglu, G. Aydin, and U. R. Acharya, "Convolutional neural networks for multi-class brain disease detection using MRI images," Computerized Medical Imaging and Graphics, vol. 78, p. 101673, 2019.

16. P. Rajpurkar, J. Irvin, K. Zhu, B. Yang, H. Mehta, T. Duan, et al., "Chexnet: Radiologist-level pneumonia detection on chest x-rays with deep learning," arXiv preprint arXiv:1711.05225, 2017.

17. F. Caobelli, "Artificial intelligence in medical imaging: Game over for radiologists?," European journal of radiology, vol. 126, 2020.

18. A. M. Alqudah, S. Qazan, and A. Alqudah, "Automated Systems for Detection of COVID-19 Using Chest X-ray Images and Lightweight Convolutional Neural Networks," 2020.

19. A. A. Ardakani, A. R. Kanafi, U. R. Acharya, N. Khadem, and A. Mohammadi, "Application of deep learning technique to manage COVID-19 in routine clinical practice using CT images: Results of 10 convolutional neural networks," Computers in Biology and Medicine, p. 103795, 2020.

20. A. Narin, C. Kaya, and Z. Pamuk, "Automatic detection of coronavirus disease (covid-19) using x-ray images and deep convolutional neural networks," arXiv preprint arXiv:2003.10849, 2020.

21. T. Ozturk, M. Talo, E. A. Yildirim, U. B. Baloglu, O. Yildirim, and U. R. Acharya, "Automated detection of COVID-19 cases using deep neural networks with X-ray images," Computers in Biology and Medicine, p. 103792, 2020.

22. S. Minaee, R. Kafieh, M. Sonka, S. Yazdani, and G. J. Soufi, "Deep-covid: Predicting covid-19 from chest x-ray images using deep transfer learning," arXiv preprint arXiv:2004.09363, 2020.

23. T. Mahmud, M. A. Rahman, and S. A. Fattah, "CovXNet: A multi-dilation convolutional neural network for automatic COVID-19 and other pneumonia detection from chest X-ray images with transferable multi-receptive feature optimization," Computers in biology and medicine, vol. 122, p. 103869, 2020.

24. I. D. Apostolopoulos and T. A. Mpesiana, "Covid-19: automatic detection from x-ray images utilizing transfer learning with convolutional neural networks," Physical and Engineering Sciences in Medicine, p. 1, 2020.
25. M. Toğaçar, B. Ergen, and Z. Cömert, "COVID-19 detection using deep learning models to exploit Social Mimic Optimization and structured chest X-ray images using fuzzy color and stacking approaches," Computers in biology and medicine, vol. 121, p. 103805, 2020.
26. P. Mooney. (2018, 5-12-2020). Chest X-Ray Images (Pneumonia). Available: https://www.kaggle.com/paultimothymooney/chest-xraypneumonia.
27. E. Deniz, A. Şengür, Z. Kadiroğlu, Y. Guo, V. Bajaj, and Ü. Budak, "Transfer learning based histopathologic image classification for breast cancer detection," Health information science and systems, vol. 6, pp. 1-7, 2018.
28. A. Çinar and M. Yildirim, "Detection of tumors on brain MRI images using the hybrid convolutional neural network architecture," Medical hypotheses, vol. 139, p. 109684, 2020.
29. C. Cortes and V. Vapnik, "Support-vector networks," Machine learning, vol. 20, pp. 273-297, 1995.
30. P. Sukumar and R. Gnanamurthy, "Computer aided detection of cervical cancer using pap smear images based on adaptive neuro fuzzy inference system classifier," Journal of Medical Imaging and Health Informatics, vol. 6, pp. 312-319, 2016.